Biotransformation of fluorophenyl pyridine carboxylic acids by the model fungus *Cunninghamella elegans*

1. Fluorine plays a key role in the design of new drugs and recent FDA approvals included two fluorinated drugs, tedizolid phosphate and vorapaxar, both of which contain the fluorophenyl pyridyl moiety.
2. To investigate the likely phase I (oxidative) metabolic fate of this group, various fluorinated phenyl pyridine carboxylic acids were incubated with the fungus *Cunninghamella elegans*, which is an established model of mammalian drug metabolism.
3. ^{19}F NMR spectroscopy established the degree of biotransformation, which varied depending on the position of fluorine substitution, and GC-MS identified alcohols and hydroxylated carboxylic acids as metabolites. The hydroxylated metabolites were further structurally characterised by NMR, which demonstrated that hydroxylation occurred on the 4' position; fluorine in that position blocked the hydroxylation.
4. The fluorophenyl pyridine carboxylic acids were not biotransformed by rat liver microsomes and this was a consequence of inhibitory action, thus the fungal model was crucial in obtaining metabolites to establish the mechanism of catabolism.

Keywords: Cytochrome P450, ^{19}F NMR, fluorine, microbial model

Introduction

The unusual physicochemical properties of fluorine, such as the small van der Waals radius, high electronegativity and the strength of the C-F bond make it a very important element in the pharmaceutical industry. Incorporation of fluorine into pharmacologically active compounds results in increased lipophilicity, improved metabolic stability and enhanced potency (Murphy and Sandford, 2015). The importance of fluorine is reflected in the numbers of new fluorinated drugs that are either on the market or in development. In 2014 the US Food and Drug Administration

approved 41 new molecular entities and of the 27 small molecules, eight contain fluorine (Jarvis, 2015). Two examples are shown in Figure 1: Sivextro® (tedizolid phosphate) is manufactured by Cubist Pharmaceuticals for the treatment of skin infections, and Zontivity® (vorapaxar) from Merck is an anti-clotting agent. Both drugs have a fluorophenyl substituted pyridyl moiety and the oxidative metabolism of this group has not been determined. Therefore, in this study the biotransformation of various fluorophenyl pyridine carboxylic acids was investigated in a fungus and microsomes to establish the phase I (oxidative) metabolites.

Cunninghamella spp. are fungi that have been used extensively as microbial models of drug metabolism for decades, in particular *C. elegans*, *C. echinulata* and *C. blakesleeana* (Asha and Vidyavathi, 2009). They are easily cultivated and have cytochrome P450 activity, which has a very broad substrate range (Murphy, 2015), thus can yield phase I (oxidative) metabolites of many drugs, including those that contain fluorine (Amadio et al., 2010, Amadio and Murphy, 2011). They also have enzymes associated with phase II (conjugative) metabolism, such as sulfotransferase, glucosyl transferase and glutathione S-transferase (Zhang et al., 1996). Furthermore, *C. elegans* can be employed in the design of fluorinated drugs, by identifying through biotransformation metabolically labile sites on non-fluorinated drug leads, which can then be modified by synthesis to contain fluorine at that specific position, thereby prolonging metabolic half-life (Bright et al., 2013, Shaughnessy et al., 2014). Amongst the many xenobiotics that *Cunninghamella* spp. can biotransform are nitrogen-containing heterocycles such as quinolone (Sutherland et al., 1994), cinnoline (Sutherland et al., 1998) and phenothiazine (Sutherland et al., 2001), and in the case of phenothiazine, the metabolites were analogous to those produced in mammals. In the present study the biotransformation of several fluorophenyl-substituted pyridine

carboxylic acids (Figure 2) by *C. elegans* was investigated, as a model of the likely phase I mammalian metabolism of drugs that contain similar functionalities, such as Sivextro and Zontivity. The catabolism of the compounds in rat liver microsomes was also investigated.

Materials and methods

Chemicals

5-Phenylpyridine-2-carboxylic acid **1** (95%) was acquired from Maybridge (Thermo Scientific). 5-(3-Fluorophenyl) pyridine-3-carboxylic acid **2**, 5-(2-fluorophenyl) pyridine-3-carboxylic acid **3**, 5-(4-fluorophenyl) pyridine-3-carboxylic acid **4**, 6-(2-fluorophenyl) pyridine-3-carboxylic acid **5**, were purchased from Sigma Aldrich.

Culture conditions

Cunninghamella elegans was cultivated on sabouraud dextrose agar for 120 h at 27 °C. Inoculum was prepared by homogenising the mycelium in sterile 0.8% NaCl (100 mL). The homogenate (5 mL) was used to inoculate 250 mL Erlenmeyer flasks containing 45 mL sabouraud dextrose broth, then incubated 72 h with rotary agitation (150 rpm) at 28 °C. The compounds were solubilised in dimethyl sulfoxide, 50 µL was added to the flask and incubation was continued for a further 24 h (unless stated otherwise). Supernatant from the biotransformation experiments was extracted in ethyl acetate; the solvent was removed under reduced pressure and the residue re-dissolved in methanol.

Isolation of biotransformation products

Organic extracts from shake flasks were analysed by reversed-phase high-performance liquid chromatography (HPLC) with a Varian prostar HPLC system equipped with Zorbax SB-C18 5 µm 4.6 × 150 mm column (Agilent technologies) and a UV–Vis

detector monitoring at 250 nm. Analytes were eluted with a gradient of acetonitrile / water (20–80 % acetonitrile) over 35 min at a flow rate of 1 mL/min. The metabolites were purified by semi-preparative HPLC with an Ascentis C18 column (15 cm×10 mm, 5 µm Supelco), with a flow rate of 4mL/min for 35 minutes eluted with a gradient of acetonitrile containing trifluoroacetic acid (0.1% v/v)/water (20-80%). Fractions containing putative metabolite as indicated by UV absorbance, were pooled and extracted in ethyl acetate. To remove residual trifluoroacetic acid, the organic extracts were back extracted in an alkaline solution (pH 11). The isolated metabolites were confirmed by GC-MS and ^{19}F NMR.

Analysis of biotransformation products

Gas chromatography–mass spectrometry analysis was routinely conducted on per trimethylsilylated extracts using an Agilent 6890 gas chromatograph coupled to a 5973 mass selective detector. Silylation was performed by adding 50 µL *N*-methyl- *N*-(trimethyl-silyl) trifluoroacetamide (MSTFA, Sigma) to a dried aliquot of the extracted supernatant and heating at 100 °C for 1 h. Derivatised samples (1 µL) were injected in the split mode onto a HP-5MS column (30 m × 0.25 mm × 0.25 µm) and the oven temperature held at 150 ^{0}C for 2 min then raised to 300 ^{0}C at 10 ^{0}C min^{-1}. The mass spectrometer was operated in scan mode. Accurate mass measurements were obtained with a LCT time-of-flight mass spectrometer (Waters Corp., USA).

^{19}F NMR, ^{1}H NMR and ^{13}C NMR spectra were recorded on Varian Inova 400 MHz or Agilent 126 and 500 MHz spectrometers with DMSO-d_6 used as the solvent. Chemical shifts (δ) are reported in ppm and coupling constants are given in Hz. ^{1}H signals were assigned using 2D homonuclear ^{1}H-^{1}H gradient COSY experiments. The ^{1}H coupling constants were determined by 1D ^{1}H spectra. ^{13}C signals were assigned using 2D heteronuclear ^{1}H-^{13}C and ^{19}F-^{13}C HSQC and ^{1}H-^{13}C HMBC experiments. The

degree of transformation was determined by ^{19}F NMR spectroscopy of the crude reaction mixture. Inversion recovery experiments were performed to measure the relaxation time of the different compounds to improve accuracy of ^{19}F NMR analysis for quantitative measurement; consequently the relaxation delay was increased to 30 seconds.

5-(3'-fluoro-4'-hydroxyphenyl) pyridine-3-carboxylic acid **8**

^{19}F NMR (376 MHz, DMSO-d_6) δ_F -135.6 (dd, J = 12.5, 9 Hz), ^{1}H NMR (400 MHz, DMSO-d_6) δ_H 10.18 (s, OH-4'), 9.03 (d, J = 2.5 Hz, H-2), 8.96 (d, J = 2 Hz, H-6), 8.36 (t, J = 2 Hz, H-4), 7.63 (dd, J = 12.5, 2.5 Hz, H-2'), 7.42 (ddd, J = 8.5, 2.5, 1 Hz, H-6'), 7.04 (dd, J = 9, 8.5 Hz, H-5'), ^{13}C NMR (126 MHz, DMSO-d_6) δ_C 151.9 (C-3'), 151.3 (C-2), 148.8 (C-6), 134.3 (C-4), 123.8 (C-6'), 118.9 (C-5'), 115.2 (C-2'), HRMS (ESI-TOF) m/z: $[M + H]^+$ Calcd for $C_{12}H_8FNO_3$ 234.0566; Found 234.0563.

5-(2'-fluoro-4'-hydroxyphenyl) pyridine-3-carboxylic acid **9**

^{19}F NMR (376 MHz, DMSO-d_6) δ_F -116.97 (dd, J = 13, 9.5 Hz), ^{1}H NMR (400 MHz, DMSO-d_6) δ_H 10.22 (s, OH-4'), 8.98 (d, J = 2 Hz, H-2), 8.87 (t, J = 2 Hz, H-6), 8.28 (q, J = 2 Hz, H-4), 7.46 (dd, J = 9.5, 8.5 Hz, H-6'), 6.75 (dd, J = 8.5, 2.5 Hz, H-5'), 6.65 (dd, J = 13, 2.5 Hz, H-3'), ^{13}C NMR (126 MHz, DMSO-d_6) δ_C 160.4 (C-2'), 152.7 (C-6), 148.8 (C-2), 136.5 (C-4), 131.7 (C-6'), 113.0 (C-5'), 103.6 (C-3'), HRMS (ESI-TOF) m/z: $[M + H]^+$ Calcd for $C_{12}H_8FNO_3$ 234.0566; Found 234.0571.

6-(2'-fluoro-4'-hydroxyphenyl) pyridine-3-carboxylic acid **10**

^{19}F NMR (376 MHz, DMSO-d_6) δ_F -114.0 (dd, J = 13.5, 9.5 Hz), ^{1}H NMR (500 MHz, DMSO-d_6) δ_H 10.40 (s, OH-4'), 9.10 (d, J = 2 Hz, H-2), 8.28 (dd, J = 8.5, 2.5 Hz, H-4),

7.91 (dd, *J* = 9.5, 8.5 Hz, H-6'), 7.82 (dd, *J* = 8.5, 2 Hz, H-5), 6.76 (dd, *J* = 8.5, 2.5 Hz, H-5'), 6.68 (dd, *J* = 13.5, 2.5 Hz, H-3'), ^{13}C NMR (126 MHz, DMSO-d_6) δ_C 161.4 (C-2'), 150.7 (C-2), 138.2 (C-4), 132.3 (C-6'), 123.2 (C-5), 112.9 (C-5'), 103.7 (C-3').

6-(2'-fluorophenyl) pyridine-3-methanol **11**

^{19}F NMR (376 MHz, DMSO-d_6) δ_F -117.44 – -117.53 (m), ^{1}H NMR (500 MHz, DMSO-d_6) δ_H 8.64 (d, *J* = 2 Hz, H-2), 7.91 (td, *J* = 8, 2 Hz, H-5'), 7.81 (dd, *J* = 8, 2.5 Hz, H-4), 7.74 (dd, *J* = 8, 2 Hz, H-5), 7.46 (tdd, *J* = 7.5, 5, 2 Hz, H-3'), 7.32 (d, *J* = 8 Hz, H-6'), 7.30 (dd, *J* = 8, 5 , H-4'), 5.35 (t, *J* = 5.5 Hz, H-8), 4.57 (d, *J* = 5.5 Hz, 2H-7), ^{13}C NMR (126 MHz, DMSO-d_6) δ_C 160.3 (C-2'), 148.7 (C-2), 135.5 (C-4), 131.1 (C-3'), 129.9 (C-5'), 125.3 (C-6'), 124.0 (C-5), 116.6 (C-4'), 60.1 (CH_2) , HRMS (ESI-TOF) m/z: [M + H]$^+$ Calcd for $C_{12}H_{10}FNO$ 204.0825; Found 204.0829.

Mammalian biotransformation

Methods employed in the transformation by rat liver microsomes were similar to that described by Obach *et al* (1998). Rat liver microsomes (1 mg/mL) were incubated for 2 hours at 37 ^{o}C with the compounds **2-5** (0.5 mM, 0.25 mM, 0.125 mM) dissolved in DMSO (0.25% v/v), plus magnesium chloride (3.3 mM) and NADPH (1 mM) in a final volume of 0.5ml sodium phosphate buffer (25 mM, pH 7). The metabolites were extracted using ethyl acetate. Extracts were derivatised and analysed by GC-MS as described above except using splitless mode with the oven temperature held at 120 ^{0}C for 2 min then raised to 300 ^{0}C at 10 ^{0}C min^{-1}. Control biotransformation experiments were conducted using flurbiprofen as the substrate. To measure the inhibition of the fluorophenyl pyridine carboxylic acids on rat liver microsomes, a co-incubation study using flurbiprofen (0.5 mM) and titrated concentrations of **2** were added as described

above. 4'-Hydroxy-flurbiprofen was detected and the transformation efficiency was determined through integration of the peaks and expressed as a percentage of the combined areas of flurbiprofen and hydroxyflurbiprofen.

Results

Biotransformation of fluorophenyl pyridine carboxylic acids

Initial biotransformation products formed after **2**-**5** were incubated with the fungus were detected by ^{19}F NMR spectroscopy (Table 1). No abiotic transformation of any of the compounds was observed. Comparison of the resonance integrals indicated that compounds **2** and **5** were extensively biotransformed to fluorometabolites after 24 h; compound **3** was poorly metabolised and compound **4** was not biotransformed. GC-MS analysis of the fungal extracts after silylation shed further light on the nature of the metabolites (Table 2). No biotransformation product was detected from **4**, which is consistent with the ^{19}F NMR analysis. A single metabolite with the expected mass of a hydroxylated carboxylic acid (**8** and **9**, Figure 3) was detected from cultures incubated with **2** and **3**, respectively. Along with a hydroxylated carboxylic acid (**6** and **10**), an additional metabolite (**7** and **11** respectively, Figure 3) was detected from extracts of fungal cultures incubated with **1** (non-fluorinated) and **5**, respectively. The mass of the derivatives was consistent with that of the (fluoro-) phenyl pyridine alcohol (**7** and **11**), and ^{1}H NMR analysis of the purified fluorometabolite **11** revealed a new doublet for methylene (δ_H 4.57 ppm, J = 5.5 Hz) and a new triplet for the –OH (δ_H 5.35 ppm, J = 5.5 Hz). Extended incubation with *C. elegans* for a further 24 h resulted in the disappearance of these metabolites and the detection of the mono-hydroxy phenyl pyridine carboxylic acids (Figure 4). Similar reduction and oxidation of carboxyl

groups has been observed in our previous study on biphenyl carboxylic acids (Bright et al., 2013).

Site of mono-hydroxylation

Our previous studies on biphenyl systems (Amadio et al., 2010, Bright et al., 2013, Shaughnessy et al., 2014) demonstrated that the hydroxylation typically occurs on the 4' (para) position. Furthermore, when this site is blocked by fluorine, no hydroxylation occurs, and the observation that **4** was not biotransformed by the fungus is consistent with this. The hydroxylated fluorometabolites **8**, **9** and **10** (Figure 4) were further purified from the culture extracts by semi-preparative HPLC and subjected to structural characterisation by NMR. This revealed that the starting substrates **2**, **3** and **5** were all hydroxylated in the expected 4' position, since the hydrogens δ_H 7.54 (**2**), 7.52 ppm (**3**) and 7.37 ppm (**5**), disappear in the hydroxylated products. This was supported by the effect of the hydroxyl group on the splitting of the fluorine signal, changing its multiplicity to a doublet of doublets in each case and furthermore, by the strong coupling (12.5-13.5 Hz) between the fluorine atoms and their respective *ortho* hydrogens. For example, the coupling of the fluorine (12.5, 9 Hz) in metabolite **8**, revealed that the hydrogen δ_H 7.63 ppm assigned to the 2' position, shared a strong $^3J_{HF}$ coupling (12.5 Hz). Whereas, its *meta* hydrogen, δ_H 7.06 assigned to the 5' position shared a $^4J_{HF}$ coupling of 9 Hz.

Mammalian biotransformation of fluorophenyl pyridine carboxylic acids

In order to compare the metabolites formed in the fungus with mammalian metabolites, compounds **2-5** were incubated with rat liver microsomes. However, no biotransformation products were detected by GC-MS. To determine if the fluorophenyl pyridine carboxylic acids are inhibitors of the microsomal preparations, various

concentrations of **2** were incubated with microsomes plus another transformable substrate, flurbiprofen. GC-MS analysis of the ethyl acetate extracts demonstrated that in the absence of **2** or at a concentration of 0.125 mM of **2**, the expected metabolite 4'-hydroxyflurbiprofen was detected, but in the presence of 0.25 mM of **2**, no metabolite was detected (Figure 5). Interestingly, when 0.125 mM of **2** was incubated with the microsomes, no biotransformation was observed, even though at this concentration the starting compound is not inhibitory to the hydroxylation of flurbiprofen.

Discussion

With the exception of the 4'-fluorinated derivative **4**, *C. elegans* biotransformed various pyridine carboxylic acids **1**- **3** and **5** to phase I (oxidative) metabolites **8**-**10** that were hydroxylated on the fluorophenyl ring. Hydroxylated metabolites have been detected from similar bicyclic aromatic compounds incubated with this fungus, but none that contain the pyridyl moiety. Indeed, pyridine-containing substrates are often biotransformed to *N*-oxides by *C. elegans* (Parshikov et al., 2012), and (Zeng et al., 2012) reported that 3-(N-Boc-aminomethyl)-5-bromopyridine was oxidized to the N-oxide by *C. echinulata*. With the substrates **1**-**5** employed in this study (Figure 2) no *N*-oxidation was observed.

The site of fluorine substitution had an influence on the extent of oxidation; thus compound **2**, in which the fluorine is at C-3', was almost entirely biotransformed after 24 h incubation with *C. elegans*, whereas compound **3** (fluorine at C-2') was biotransformed to a much lesser degree and compound **4** (fluorine at C-4') was not biotransformed at all. Based on our previous studies with the related substrates fluorobiphenyl (Amadio and Murphy, 2010, Bright et al., 2013) and flurbiprofen (Amadio et al., 2010, Shaughnessy et al., 2014), the 4' position is predominantly hydroxylated and if replaced with fluorine, no hydroxylation is observed, which would

account for the absence of hydroxylation of **4**. Furthermore, **2**, **3** and **5** were similarly regiospecifically hydroxylated at C4' by the fungus.

Some researchers have correlated the regiospecificity of cytochrome P450-catalysed hydroxylation of aromatic compounds with calculated frontier orbital density distribution (Koerts et al., 1997, Rietjens et al., 1993). Here, calculated frontier orbital density distributions at high-level computations (see supporting information for details) confirm the regiospecificity of CYP-catalysed hydroxylation for compounds **1**-**3** and **5** where the highest HOMO densities are found at the 4' carbon sites in these starting molecules. Interestingly, the calculated atomic charges (Table S1) for C4' of all the substrates reveal that compound **2** has the highest negative charge, which might account for this compound being most readily hydroxylated (Table 1).

The site of phenyl ring substitution on pyridyl seems to determine whether the carboxyl is reduced, as in compounds **1** and **5**, where the phenyl is *para* to the carboxyl group and yielded the corresponding alcohol after 24 h incubation. Only the carboxylic acid is observed after 48 h, thus the alcohol is re-oxidised. None of the other compounds (**2**-**4**), which had fluorophenyl substituents *meta* to the carboxyl group, were reduced in this way. Interestingly, fluorinated biphenyl-4-carboxylic acids underwent similar reduction and re-oxidation of the carboxylate when incubated with *C. elegans* (Bright et al., 2013), but the hydroxylated alcohols were also detected as intermediates, whereas with the **1** and **5**, only the hydroxylated carboxylic acids were identified. It is likely that a carboxylate reductase, which has been identified in other fungi (Winkler and Winkler, 2016, Ma et al., 2011) and requires ATP and NADPH as co-substrates, is responsible for the reduction. It is conceivable that as incubation time progresses and in the absence of any added nutrient, the redox balance in the cell results in the reverse reaction dominating, thus the carboxylic acid is produced.

Rat liver microsomes were unable to transform any of the fluorophenyl pyridine carboxylic acids, most likely because these compounds are inhibitors of the CYPs present. Pyridine inhibits rabbit liver microsomes (Kaul and Novak, 1987) and interestingly the *N*-oxide metabolite is formed, but no such metabolite was observed with **2**. It is possible that the whole cells of *C. elegans* are more resilient to the inhibitory effects of the substrates in comparison to microsomes, which underscores the effectiveness of the fungal system as a mammalian proxy for *in vitro* assessment of xenobiotic biotransformation.

Studies of the human metabolism of voraxapar and tedizolid phosphate have revealed that the drugs are not degraded to a point where fluorophenyl pyridine is formed as a discrete metabolite (Ghosal et al., 2011; Ong et al., 2014). Nevertheless, it is likely that this structural motif will be incorporated into future pharmaceutical agents, thus understanding the likely phase I metabolism arising from related model compounds, such as **2**-**5**, will help in the prediction of the likely metabolites formed.

Conclusions

This study demonstrates that *Cunninghamella elegans* is able to produce hydroxylated metabolites of fluorophenyl pyridine carboxylic acids, and that the extent and regioselectivity of hydroxylation is dependent on the position of the fluorine substituent. The absence of biotransformation products in microsomal incubations illustrates the usefulness of the fungus in generating difficult-to-obtain metabolites of relevant xenobiotics and drug-like molecules to enable a comprehensive understanding of their metabolism.

Supporting Information

Computational details on compounds **1**-**11** including calculated frontier orbital densities and atomic charges of carbon atoms for **1**-**5** and ^{19}F GIAO-NMR shifts for **2**-**5** and **8**-**11**.

Declaration of interest

The authors declare not conflict of interest.

References

Amadio J, Gordon K, Murphy CD. (2010). Biotransformation of flurbiprofen by *Cunninghamella* species. Appl Environ Microbiol 76: 6299-6303.

Amadio J, Murphy CD. (2010). Biotransformation of fluorobiphenyl by *Cunninghamella elegans*. Appl Microbiol Biotechnol 86: 345-351.

Amadio J, Murphy CD. (2011). Production of human metabolites of the anti-cancer drug flutamide via biotransformation *in Cunninghamella species*. Biotechnol Lett 33: 321-326.

Asha S, Vidyavathi M. (2009). *Cunninghamella* - A microbial model for drug metabolism studies - A review. Biotechnol Adv 27: 16-29.

Bright TV, Dalton F, Elder VL, Murphy CD, O'Connor NK, Sandford G. (2013). A convenient chemical-microbial method for developing fluorinated pharmaceuticals. Org Biomol Chem 11: 1135-1142.

Ghosal A, Xiaowen L, Penner N, Gao L, Ramanathan R, Chowdhury SK, Kishnani NS, Alton KB (2011) Identification of human liver cytochrome P450 enzymes involved in the metabolism of SCH 530348 (vorapaxar), a potent oral thrombin protease-activated receptor 1 antagonist. Drug Metab Dispos 39: 30-38.

Jarvis L (2015) The year in new drugs. Chem Engin News 93: 11-16.

Kaul KL, Novak RF. (1987). Inhibition and induction of rabbit liver microsomal cytochrome P450 by pyridine. J Pharmacol Exp Ther 243: 384-390.

Koerts J, Verlaeds MC, Soffers A, Vervoort J, Rietjens I. (1997). Influence of substituents in fluorobenzene derivatives on the cytochrome P450-catalyzed hydroxylation at the adjacent *ortho* aromatic carbon center. Chem Res Toxicol 10: 279-288.

Ma L, Liu X, Liang J, Zhang Z. (2011). Biotransformations of cinnamaldehyde, cinnamic acid and acetophenone with *Mucor*. World J Microbiol Biotechnol 27: 2133-2137.

Murphy CD. (2015). Drug metabolism in microorganisms. Biotechnol Lett 37: 19-28.

Murphy CD, Sandford G. (2015). Recent advances in fluorination techniques and their anticipated impact on drug metabolism and toxicity. Expert Opinion on Drug Metabolism & Toxicology 11: 589-599.

Obach RS. (1999). Prediction of human clearance of twenty-nine drugs from hepatic microsomal intrinsic clearance data: An examination of in vitro half-life approach and nonspecific binding to microsomes. Drug Metab Dispos 27: 1350-1359.

Ong V, Flanagan S, Fang E, Dreskin HJ, Locke JB, Bartizal K, Prokocimer P (2014) Absorption, distribution, metabolism, and excretion of the novel antibacterial prodrug tedizolid phosphate. Drug Metab Dispos 42: 1275-1284.

Parshikov IA, Netrusov AI, Sutherland JB. (2012). Microbial transformation of azaarenes and potential uses in pharmaceutical synthesis. Appl Microbiol Biotechnol 95: 871-889.

Rietjens I, Soffers A, Veeger C, Vervoort J. (1993). Regioselectivity of cytochrome P450 catalyzed hydroxylation of fluorobenzenes predicted by calculated frontier orbital substrate characteristics. Biochemistry 32: 4801-4812.

Shaughnessy MJ, Harsanyi A, Li JJ, Bright T, Murphy CD, Sandford G. (2014). Targeted fluorination of a nonsteroidal anti-inflammatory drug to prolong metabolic half-life. ChemMedChem 9: 733-736.

Sutherland JB, Freeman JP, Heinze TM, Moody JD, Parshikov IA, Williams AJ, Zhang D. (2001). Oxidation of phenothiazine and phenoxazine by *Cunninghamella elegans*. Xenobiotica 31: 799-809.

Sutherland JB, Freeman JP, Williams AJ and Cerniglia CE (1994) N-oxidation of quinoline and isoquinoline by *Cunninghamella elegans*. Exp Mycol 18: 271-274.

Sutherland JB, Freeman JP, Williams AJ, Deck J. (1998). Metabolism of cinnoline to N-oxidation products by *Cunninghamella elegans* and *Aspergillus niger*. J Indust Microbiol Biotechnol 21: 225-227.

Winkler M, Winkler CK. (2016). *Trametes versicolor* carboxylate reductase uncovered. Monatshefte Fur Chemie 147: 575-578.

Zeng J, Gage D, Zhan J. (2012). Production of a new pyridine N-oxide by bioconversion with *Cunninghamella echinulata* var. *elegans*. J Biosci Bioengin 114: 497-499.

Zhang DL, Yang YF, Leakey JEA, Cerniglia CE. (1996). Phase I and phase II enzymes produced by *Cunninghamella elegans* for the metabolism of xenobiotics. FEMS Microbiol Lett 138: 221-226.

Table 1. ^{19}F NMR analysis of the biotransformation products **8**-**11** from compounds **2**-**5** in *C. elegans*. The observed ^{19}F NMR shifts are in excellent agreement with predicted GIAO-NMR shifts (see supporting information).

Compound	Substrate δ_F (ppm)	Fluorometabolite(s) δ_F (ppm)	Compound	Yield
2	-112.5	-135.6	**8**	95%
3	-118.6	-116.9	**9**	22%
4	-113.2	N.D.		
5	-116.7	-114.0, -117.5	**10**, **11**	36%, 59%

N.D. Not detected

Table 2. GC-MS analysis of silylated substrates and metabolites from the biotransformation of compounds **1-5** by *C. elegans*. Each –OH group in compounds (**1-11**) is replaced by a $–OSiMe_3$ group after silylation.

Compound	t_R (min)	*m/z* M^+	Metabolite t_R (min)	Metabolite *m/z* M^+
1	10.75	271	9.18, 14.16	257, 359
2	9.89	289	13.33	377
3	9.93	289	13.26	377
4	10.04	289	N.D.	N.D.
5	10.15	289	9.45, 13.62	275, 377

Figure 1

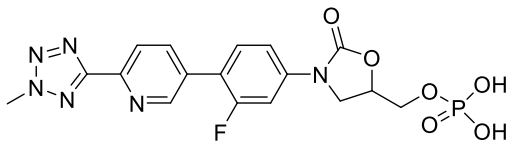

Sivextro

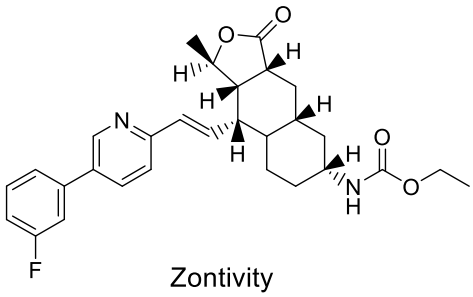

Zontivity

Figure 2

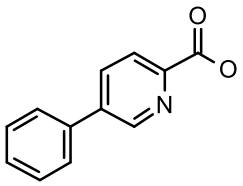

1

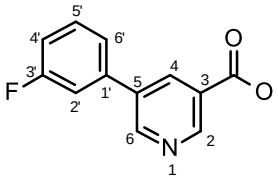

2

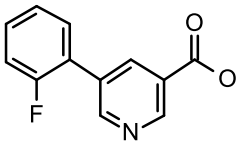

3

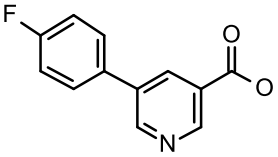

4

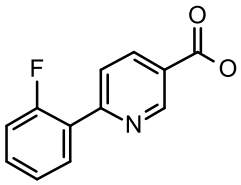

5

Figure 3

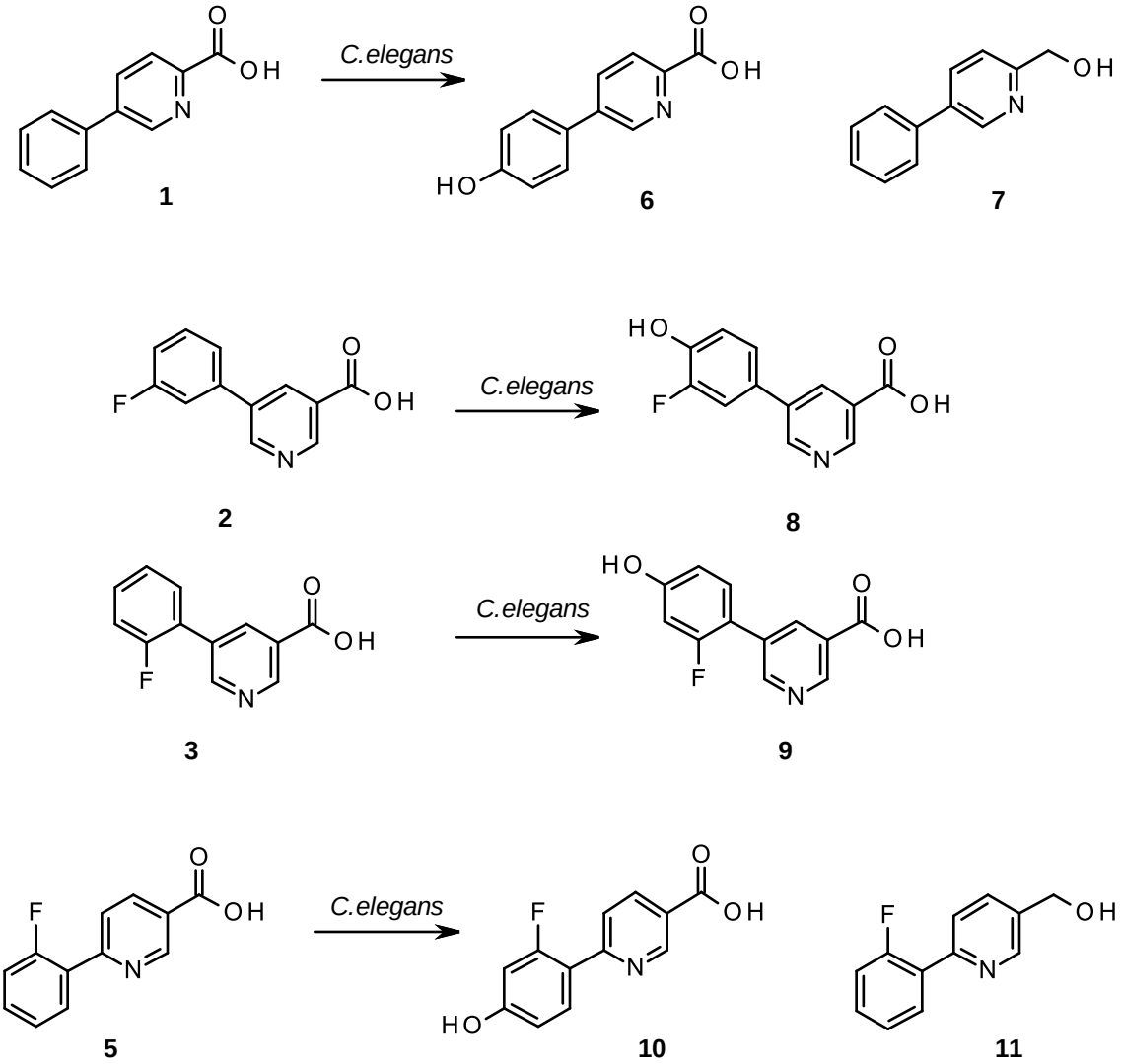

Figure 4

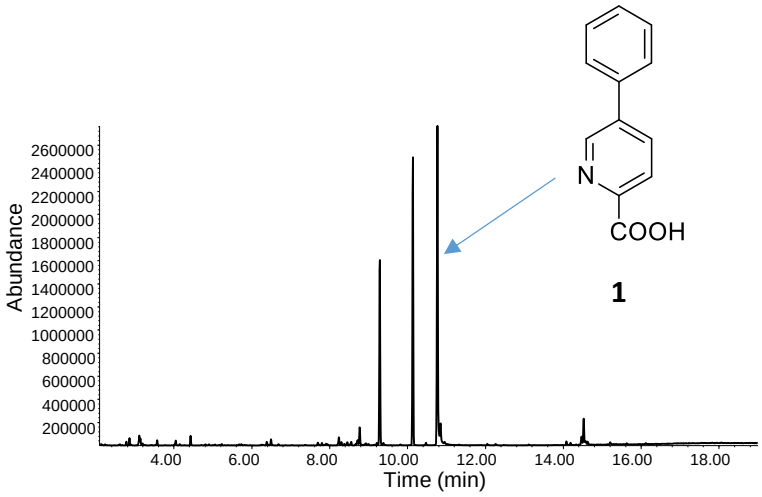

Time= 0

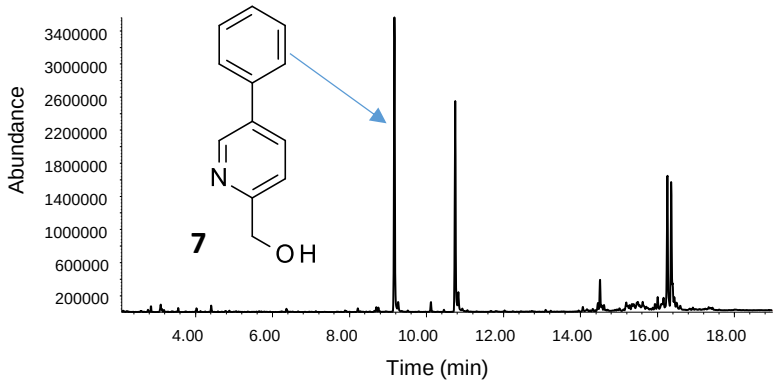

Time= 24 h

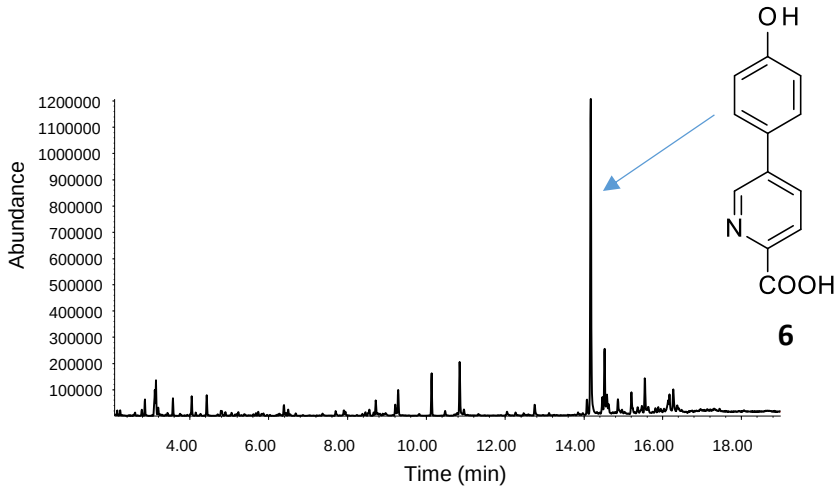

Time= 48 h

Figure 5

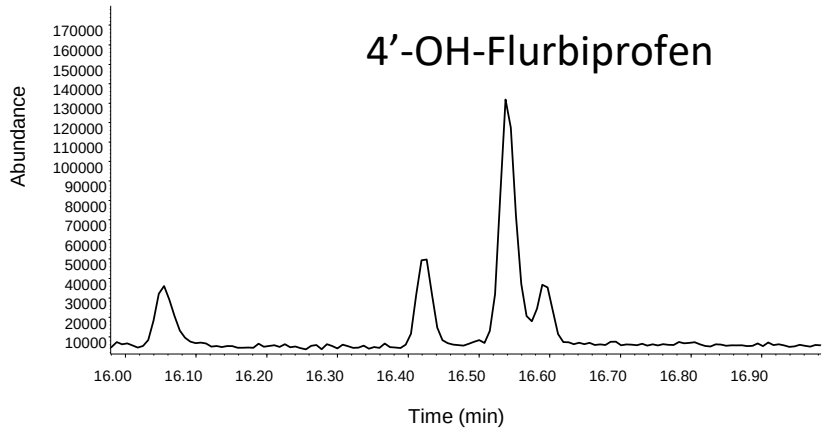

0 mM **2**

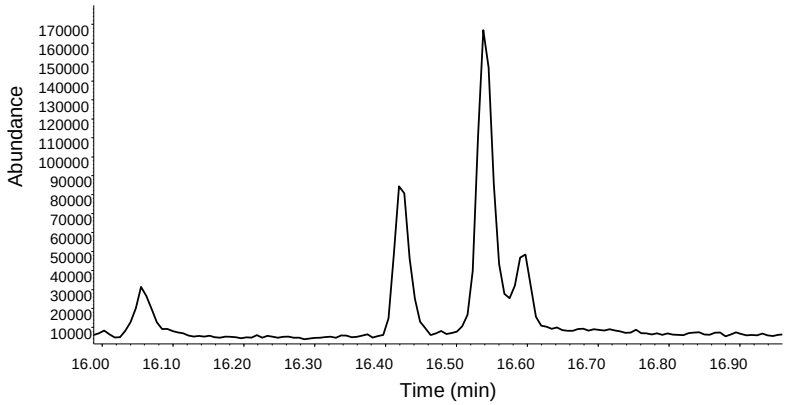

0.125 mM **2**

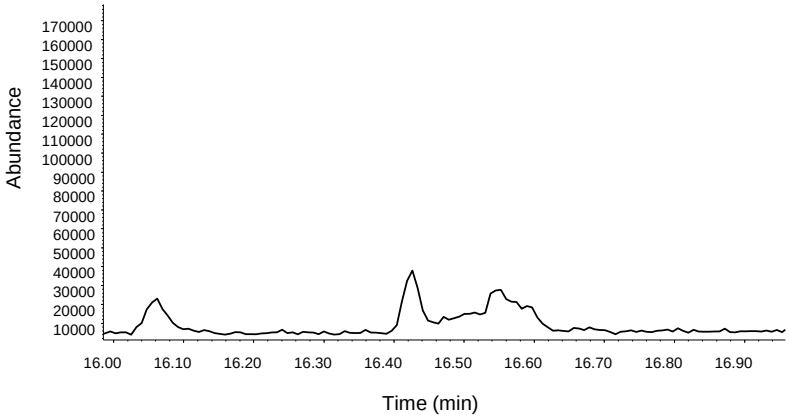

0.25 mM **2**

Figure captions

Figure 1. Structures of the recently FDA-approved fluorinated drugs Sivextro and Zontivity.

Figure 2. Structures of the pyridine carboxylic acids **1**-**5** used in this study.

Figure 3. Hydroxylated biotransformation products **6**-**11** formed upon incubation of pyridine carboxylic acids **1**, **2**, **3** and **5**. The site of hydroxylation of **6** was predicted based on the other biotransformation products and GC-MS data.

Figure 4. Total ion chromatograms of the biotransformation products **6** and **7** from **1** after different incubation periods.

Figure 5. Total ion chromatograms of the 4'-hydroxylated microsomal biotransformation product of flurbiprofen formed in the presence of various concentrations of **2**.